NUMERICAL CORRECTION FOR THE DIFFUSE SOLAR IRRADIANCE BY THE MELO-ESCOBEDO SHADOWRING MEASURING METHOD

Alexandre Dal Pai[1], João Francisco Escobedo[2] and Fábio Henrique Pires Corrêa[2]

[1] Faculdade de Tecnologia/CENTRO PAULA SOUZA, Botucatu (Brazil)

[2] Faculdade de Ciências Agronômicas/UNESP, Botucatu (Brazil)

1. Abstract

The present paper deals with numerical corrections factors proposed as a function of the clearness index in order to correct the diffuse solar irradiance measured with the Melo-Escobedo Shadowring Measuring Method (ME shadowring). The global irradiance was measured by an Eppley - PSP pyranometer ; direct normal irradiance by an Eppley-NIP pyrheliometer fitted to a ST-3 sun tracking device and the diffuse irradiance by an Eppley-PSP pyranometer fitted to a ME shadowring. The validations were performed by the MBE and RMSE statistical indicators. The results showed that the numerical correction factors were appropriate to correct the shadowring diffuse irradiance.

2. Introduction

Among the solar radiation components used in meteorological stations observed in the world, global radiation on horizontal surface is the most extensively quantity measured. However, measurements of diffuse and direct radiations are less common. A monitoring station typically measures only two of the insolation components and calculates the other. The global and diffuse components are often measured. The direct irradiation is calculated through the Eq. (1) (global I_G radiation is the sum of the diffuse I_d and direct $I_{b,h}$ radiations) due to the expensive maintenance , associated with solar tracking for the direct normal measurement.

$$I_G = I_d + I_{b,h} \qquad \text{(eq 1)}$$

The shadowing method is adopted in the measurement of diffuse radiation. In this method, which presents low costs, easy maintenance and optimal operation, the ring is oriented perpendicularly to the polar axis and at an angle equal to the local latitude. It shades the bands center point from sunrise to sunset. An instrument is placed at this point and it permits the measurement of diffuse radiation for extended periods of time.

Drummond (Drummond, 1956) and Robinson (Robinson and Stoch, 1964) (Fig. 1) are two well-known shading setups. In Drummond´s setup, the pyranometer is fixed and the shadowring is translated parallelly to the polar axis which acts to compensate the solar declination. This means that periodical mechanical adjustments are necessary. In this setup, the shadowring, as seen from the pyranometer, varies its width and distance with the solar declination. In Robinson´s setup, the pyranometer is fixed in the center of the shadowring and the shadowring is rotated around its center to compensate the solar declination. The width and the distance do not change in this setup.

An alternative shadowring setup was proposed by Melo & Escobedo (1994) - ME shadowring (Fig. 1). In this setup , mechanical operation is inverse to Drummond's setup. In the ME setup, the shadowring is fixed and the pyranometer is translated parallelly to the local horizon plan in a mobile base to compensate the solar declination.

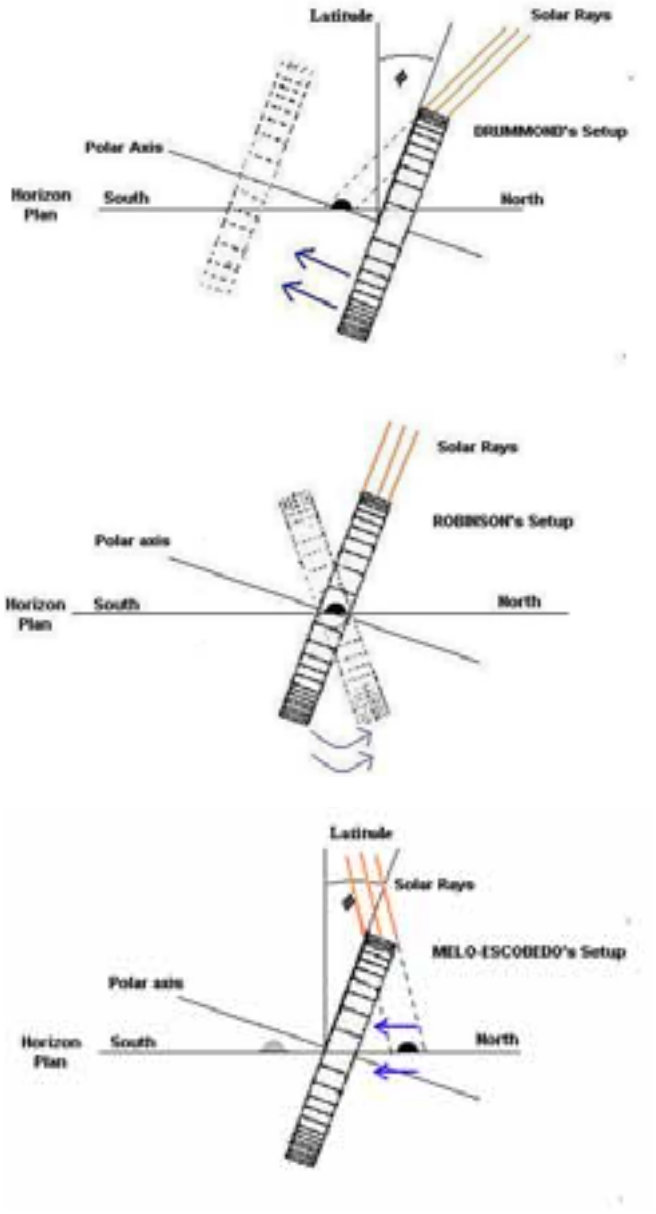

Fig 1 – Shadowring setups: Drummond, Robinson-Stoch and Melo-Escobedo.

A drawback of the shadowring method is the use of correction factors (FC) to compensate the diffuse irradiance blocked by the shadowring (Drummond, 1956; Kasten et al, 1983; Dehne, 1984; Ineichen et al, 1984; Stanhill, 1985) given by the Eq. (2). The loss fraction (Fp) is based on the isotropy of the radiation, which is considered a geometric function (the ring length and width) and geographical factors(latitude and solar declination). Oliveira et al (2002) calculated the loss fraction for the ME shadowring (Eq. (3)).

$$FC = \frac{1}{1 - F_P} \qquad \text{(eq 2)}$$

$$F_P = \left(\frac{2b}{\pi R}\right).\cos(\delta).\left[\frac{\cos(\phi + \delta)}{\cos(\phi)}\right]^2 .\int_0^{w_s} \cos(\Theta_Z)dw \qquad \text{(eq 3)}$$

where b is the ring width, R the radius of the ring, δ the solar declination, ϕ the latitude, ω the hourly angle and Θ_Z the zenital angle.

The use of the isotropic correction doesn't take into account the atmospheric effects (turbidity, cloudiness,

pollution, water vapor) that are responsible for the anisotropy of the diffuse radiation. Kasten et al. (1983) and Pollard and Langevine (1988) introduced corrections based on anisotropic parameters such as clearness index K_T (ratio of global to extraterrestrial radiation), zenital angle and turbidity atmospheric to improve the precision of the shadowring diffuse irradiance. Dehne (1984) observed that the anisotropic corrections are local dependent, while Painter (1981) and Stanhill (1985) verified that the anisotropic seasonal corrections are dependent due to the different sizes and levels of the aerosol concentration in the atmosphere. LeBaron et al (1990) combined one isotropic (geographical) and three anisotropic parameters (zenital angle, clearness index and brightness) to develop anisotropic corrections for the shadowring diffuse irradiance. They concluded that the clearness index is the best representative parameter of the anisotropic conditions of the sky. In that direction, Drummond (1956) recommends different anisotropic corrections as a function of the clearness index: 3% for $0 < K_T < 0{,}30$, 5% $0{,}30 < K_T < 0{,}65$ and 7% for $0{,}65 < K_T < 1$. Battles et al (1995) used the same parameters of LeBaron. These authors developed two correction equations: the first is used for all parameters in an unique equation, while the second is used on geometric, zenital angle and brightness parameters as a function of four clearness index intervals. The present paper deals with numerical corrections factors proposed as a function of the clearness index in order to correct the diffuse solar irradiance measured with the Melo-Escobedo Shadowring Measuring Method (ME shadowring).

3. Methodology

3.1. Local and Climate

The present study is based upon measurements recorded by the Solar Radiometric Laboratory during the years 1996 to 2005. To develop the numerical corrections, we used four-fifth of the data, while the one-fifth remaining was used for validation purposes. The Solar Radiometric Laboratory is located on the Botucatu Campus of the Sao Paulo State University (22 54'S, 48 27'W, 716 m). Botucatu (Fig. 2) is a semi-rural town surrounded by sugar cane and eucalyptus crops with 127,328 inhabitants, few industries and the economy based upon services.

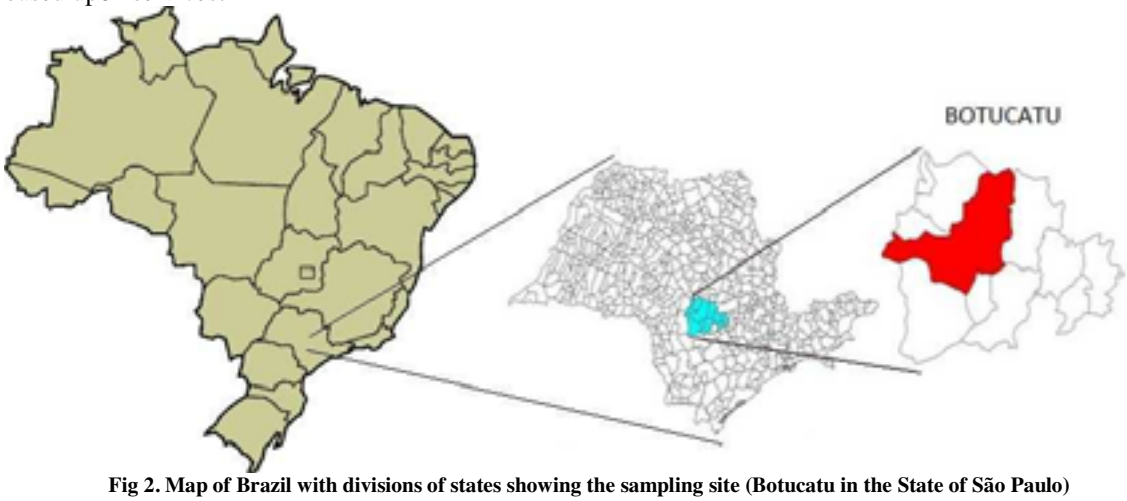

Fig 2. Map of Brazil with divisions of states showing the sampling site (Botucatu in the State of São Paulo)

According to Köppen climate classification the local climate is classified as Cwa (humid subtropical climate - mesothermal) with hot and humid summers and dry winter. Fig 3 shows monthly mean values for air temperature, relative humidity, sunshine duration and precipitation for a 35 years database. The air temperature and relative humid values follow the solar astronomical variations and the maximum and minimum values are 23,12 °C (February) and 17,10 °C (July) for air temperature and 78,25% (February) and 63,97% (August) for relative humid, respectively.

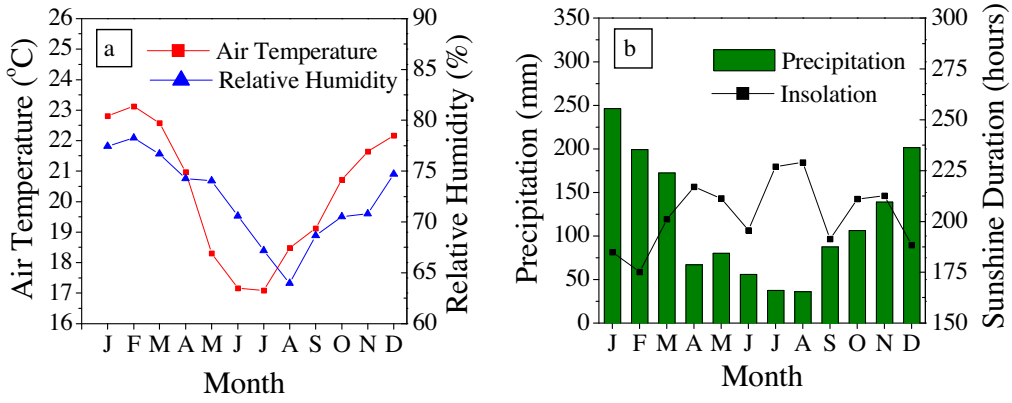

Fig 3. Annual variation of the monthly average daily values for a 35 years database. a) Air temperature and relative humidity. b) Sunshine duration and precipitation.

The rainy season occurs in the summer and spring, when there are more than 80% of the total annual rainfalls with maximum value in January (246,2 mm). In this period the rainfall is convective and caused by intense evaporation of wet and heated surfaces. These rains occur mainly in the afternoons and early evenings, they are located with great spatial variability, their intensity is moderate to strong, and the duration is short. In the dry season (winter and autumn), the monthly-mean precipitation is less than 100 mm with minimum value in August (36.10 mm). In this period the rainfall is frontal caused by the meeting of cold and dry masses from the south with the warm and humid masses from the Amazon region. The warm mass being less dense than the cold one starts to rise into the atmosphere, thus suffering adiabatic cooling. When air goes above the point of dew formation and is no longer able to hold all its water within, it begins to condense and form clouds that lead to precipitation. This rain falls over a wide area, the intensity is low to moderate and the duration is long (hours or days) depending on the speed of the front. For sunshine duration values, despite an increased photoperiod, summer months showed values less than 200 hours with a minimum in February (175,1 hours) due to cloud cover characteristic of the period. As the summer months are hot and humid, the cloud activity is intense, thus minimizing the hours of sunshine. For the winter months, the numbers of clear days is greater consequently increasing the monthly hours of sunshine with a maximum in August (229 hours). June showed a local minimum due to the cold fronts from the south that increases the cloudiness.
With regard to aerosols emitted into the atmosphere, industries and motor vehicles are the main emitters of particulate matter. However, the study area is surrounded by 70 cities that release large amounts of particulate matter as a result of burning of sugar cane, especially in the winter. According to Codato et al (2008), the highest aerosol concentration occurs in this period due to lack of rainy days, thus preventing the deposition of particulate matter.

3.2. Instrumentation, Quality Control Procedure and Statistical Error Tests

The solar global irradiance I_G was measured by an Eppley - PSP pyranometer (K = 7,45 Vm^2/W); the solar direct normal irradiance I_b by an Eppley-NIP pyrheliometer (K = 7,59 Vm^2/W) fitted to a ST-3 sun tracking device; and the solar diffuse irradiance I_{dM} by an Eppley-PSP pyranometer (K = 7,47 V/Wm-2) fitted to a ME shadowring (radius of 0,40m and width of 0,10m). Tab 1 shows the operating features of the measuring devices.

Tab 1. Operating features of the global, beam and diffuse solar irradiances measuring devices.

Irradiance	**Global**	**Direct**	**Diffuse**
Sensor-marca	Eppley Precision Spectral Pyranometer	Eppley Normal Incidence Pyrheliometer	Eppley Precision Spectral Pyranometer
Sensivity	±7,45 $\mu V/Wm^2$	7,59 $\mu V/Wm^2$	±7,47 $\mu V/Wm^2$
Spectral Range	295 – 2800 nm	295 – 2800 nm	295 – 2800 nm
Response Time	1 s	1 s	1 s
Linearity	±0,5% (from 0 to 2800 W/m^2)	±0,5% (from 0 to 1400 W/m^2)	±0,5% (from 0 to 2800 W/m^2)

Cosine	±1% (0º<Z<70º) ±3% (70º≤Z<80º)	–	±1% (0º<Z<70º) ±3% (70º≤Z<80º)
Temperature Dependence	±1% (from -20ºC to +40ºC)	±1% (from -20ºC to +40ºC)	±1% (from -20ºC to +40ºC)

Source: The Eppley Laboratory (http://www.eppleylab.com)

The diffuse irradiance data was isotropically corrected using the ME Shadowring correction factors proposed by Oliveira et al (2002) given by (eq. 2) and (eq. 3):
The true diffuse irradiance henceforth called reference diffuse irradiance I_d was calculated by the difference between the global and horizontal direct irradiances given by (eq. 4):

$$I_d = I_G - I_B \cos(Z) \quad \text{(eq. 4)}$$

The numerical corrections was based on the clearness index Kt. The clearness index is the ratio of global to extraterrestrial irradiance I_o and express the total irradiance that reaches the surface from the total available on the top of the atmosphere. The (eq. 5) and (eq. 6) shows the clearness index and the extraterrestrial irradiance I_o respectively.

$$K_T = \frac{I_G}{I_O} \quad \text{(eq. 5)}$$

$$I_O = 1367.E_O.\cos(Z) \quad \text{(eq. 6)}$$

where E_o is the orbital eccentricity. The clearness index Kt has also been used to classify the sky coverage. Tab 2 shows the Escobedo sky coverage classification (Escobedo et al, 2009) used in this work.

Tab 2. The clearness index Kt intervals and the sky coverage according to Escobedo sky coverage classification. (Escobedo et al, 2009).

Kt intervals	Sky Coverage
0 ≤ Kt < 0,35	overcast sky
0,35 ≤ Kt < 0,55	partially cloudy sky
0,55 ≤ Kt < 0,65	partially clear sky
0,65 ≤ Kt < 1	clear sky

A Campbell Scientific datalogger model Cr23X was used to monitor and to store the solar irradiance data. The values were scanned at 5 s intervals and average values at 5 min intervals were calculated and stored. Every morning values were transmitted to a computer via a storage module model SM-192.
From the 525592 data available in the ten years of measurements, 47725 of them (representing 9,09% of the total) were removed due to the application of the filters shown in Tab 3 (Kudish and Evseev, 2008). The cut values are due to misalignment, damaged wires, lack of electricity and shadowring internal reflections due to low solar altitude.

Tab 3. Quality control filters and results (Kudish and Evseev, 2008).

Solar Irradiance Type	Filter	5 min data removed (%)
Global	$I_G < I_O$	1577 (0,30%)
Normal Incident Beam	$I_b \leq I_{SC}$	27384 (5,22%)
Shadowring Diffuse	$0,1\ I_G \leq I_{dM} < I_G$	6307 (1,20%)
Reference Diffuse	$0 \leq I_d \leq I_{SC}$	12457 (2,37%)
All filters together	--	47725 (9,09%)

The evaluation of the numerical corrections was based on mean bias error MBE and root means square error RMSE statistical indicators given by the (eq. 7) and (eq. 8) respectively.

$$MBE = \left(\sum_i^N (y_i - x_i) \Big/ N \right) \quad \text{(eq. 7)}$$

$$RMSE = \left(\sum_i^N (y_i - x_i)^2 \Big/ N \right)^{1/2} \quad \text{(eq. 8)}$$

where y_i is the correct values, x_i the measured values and N the number of observations. The MBE provide information on the long-term performance of a model. A positive value means an overestimation whereas a negative one means an underestimation. A drawback of this indicator is that overestimation of an individual observation will cancel underestimation in a separate observation. The RMSE provide information on the short-term performance of a model by allowing a term by term comparison of the actual difference between the estimated value and the measured value. While a high value means a large scattering, a low one means small scattering. A drawback of this indicator is that a few large errors in the sum can produce a significant increase in RMSE.

4. Results and Discussion

4.1.All Sky Numerical Corrections

Fig 4a shows the correlation between reference diffuse irradiance and shadowring diffuse irradiance for 10 years under all sky covers. High scattering between both irradiances is due to a 5-minute mean partition. Shorter partitions respond faster to atmospheric dynamics, thus justifying the high scattering (Suehrcke & McCormick, 1988). Despite the linearity displayed, shadowring diffuse values, on average, were 4.6% lower than reference values, i.e., shadowring vales require a further correction of 1.046. This correction represents an average of 10 years of measurements and therefore considers different atmospheric situations. For a more punctual characterization, the ratio between reference and shadowring diffuse was calculated annually and is shown in Fig 4b.

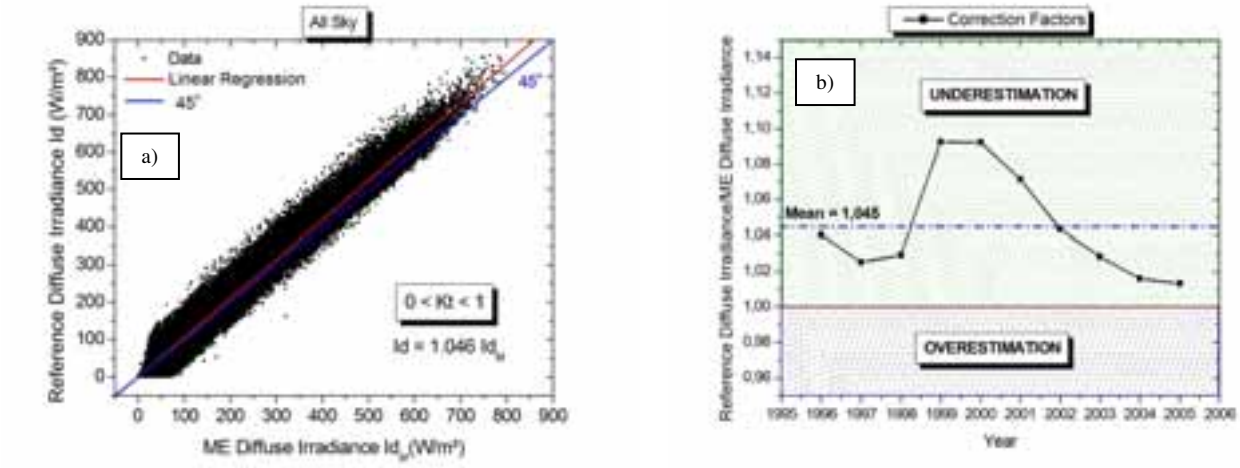

Fig 4. Correlation between reference diffuse irradiance and shadowring diffuse irradiance for 10 years under all sky conditions.

We can see that ratio values between reference and shadowring diffuse were above 1 for all years, showing that shadowring diffuse irradiance is smaller than reference diffuse irradiance, i.e., the shadowring method underestimated the measure of diffuse irradiance in all years. The variation range from 1.013 to 1.092 of these ratios is due to spatial and temporal variation of atmospheric constituents, such as clouds, water vapor, aerosols, among others. Variable distribution and quantity of these constituents change the scattering and absorption profile of solar radiation by the atmosphere and are not covered by the shadowring method, which justifies the annual variation found between reference and shadowring diffuse irradiance values. Whereas the underestimated diffuse irradiance value measured shows that the application of isotropic correction is not sufficient to correct the portion of irradiance intercepted by the shadowring, suggesting the need for additional numerical corrections dependent on atmospheric conditions.

4.2.Sky Cover Numerical Corrections

To better characterize atmospheric effects on the measurement of diffuse irradiance, according to Table 2, sky coverage was divided into four discrete intervals considering the clearness index Kt. Kt values near zero indicate a situation of low atmospheric transmissivity due to large cloud concentration. On the other hand, Kt

values near 1 indicate high transmissivity due to clear sky conditions. Fig 5 shows the correlation between reference and shadowring diffuse irradiance for overcast sky.

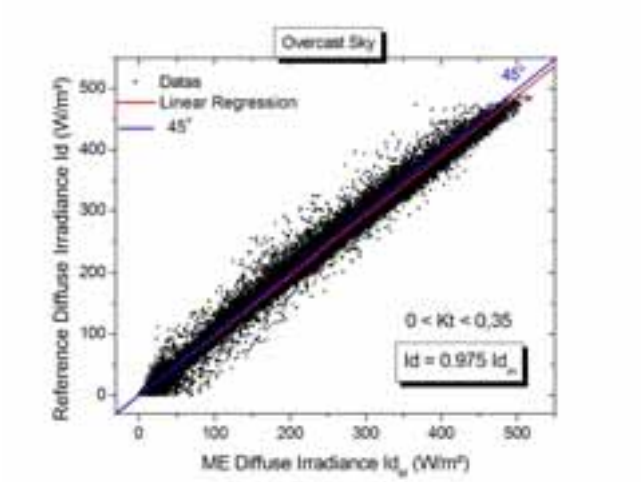

Fig 5. Correlation between reference and shadowring diffuse irradiance for overcast sky.

We can see that the linear regression is slightly below the ideal line (45º). The slope of 0.975, down 2.5% regarding the slope of the ideal line, indicates that the shadowring diffuse irradiance is greater than the reference value. Therefore, the use of the shadowring method was responsible for a 2.5% average increase in diffuse irradiance values for overcast skies. This overestimation can be explained by the climatic characteristics of Botucatu and the use of isotropic correction inherent to the shadowring method adopted. Fig 6a shows the percentage of occurrence of cloudy skies for 10-year measurements while Fig 6b shows the isotropic correction factors for Drummond's and Melo-Escobedo's shadowring devices.

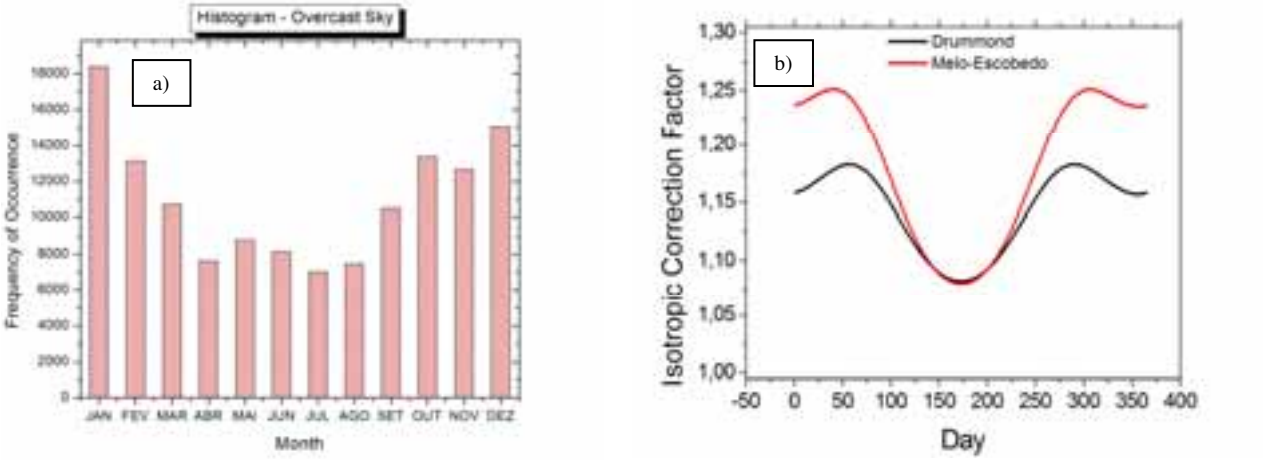

Fig 6. a) Percentage of occurrence of cloudy skies for 10-year measurements. b) Isotropic correction factors for Drummond's and Melo-Escobedo's shadowring devices.

.

Both Koppen's classification and Figure 6a indicate a higher occurrence of overcast skies in the spring and in the summer. During this period the largest isotropic corrections for ME shadowring are made, as shown in Figure 6b, with a maximum value of 25% in February and November. However, for this coverage, isotropic corrections should be less significant, as clouds themselves function as a shading device, like the ring, thus eliminating its use. Therefore, the application of isotropic correction factors for this sky coverage causes an average increase of 2.5% in shadowring diffuse irradiance measurements. Therefore, to correct this method's limitations in this coverage, we propose the correction of diffuse irradiance by 2.5%, multiplying it by the average factor 0.975. Drummond (1956) suggests that the use of his shadowring causes an underestimation of 3%, unlike the overestimation of 2.5% provided by the ME shadowring. This is probably due to smaller isotropic correction factors used by Drummond's shadowring.

By way of comparison, Fig 7 shows reference and shadowring diffuse irradiances in the months of January (summer) and July (winter), characterized by a greater and smaller overcast sky cover, respectively.

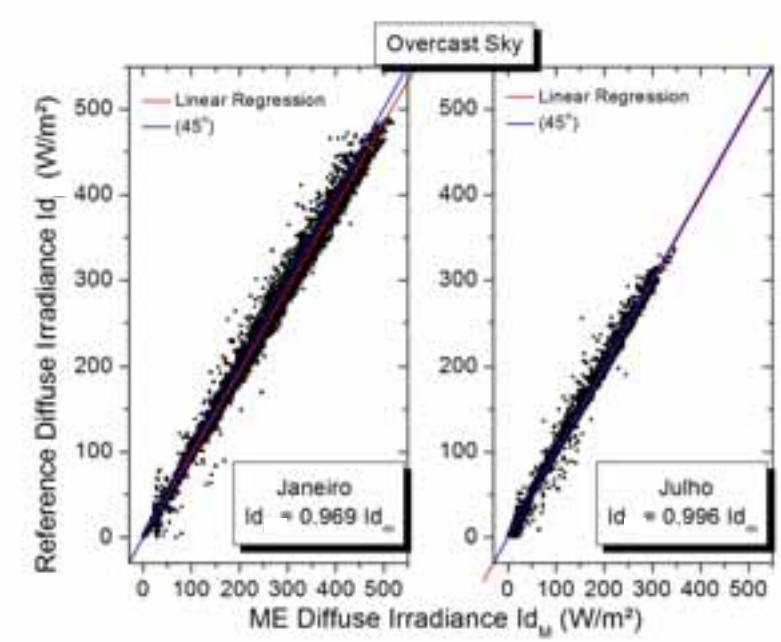

Fig 7. Reference and shadowring diffuse irradiances in the months of January (summer) and July (winter)

January had the highest overestimation of diffuse irradiance (a 3.1% increase), whereas the overestimation in July was only 0.4%. Therefore, for overcast sky cover, the use of the shadowring method, on average, overestimates the measure of diffuse irradiance and needs correcting owing to sky cover, especially in the spring and summer.

Set in the range from 0.35 to 0.65 Kt, partially overcast sky cover is characterized as a transition phase between overcast and clear cover, a fact that makes its characterization more difficult owing to atmospheric dynamics. Since the frequency of measure acquisition was based on an average of 60 readings in a 5-minute time span, it is likely that overcast and clear sky events were computed simultaneously, making relevant coverage analysis more difficult. In this case, seeking to better characterize atmospheric effects, partially overcast sky coverage was divided into two other sub-intervals owing to the intensity of diffuse and direct irradiances: diffuse partly cloudy and direct partly cloudy covers. The first is set to range from 0.35 to 0.55 Kt, characterized by an average diffuse irradiance greater than direct irradiance. Whereas the second, set to range from 0.55 to 0.65 Kt, is characterized by an average direct irradiance higher than diffuse irradiance. The Kt = 0.55 point separates both coverage and means that, of the 55% radiation transmission by the atmosphere, half is due to diffuse irradiance and the other half is due to direct irradiance. Fig 8a and 8b show the correlations between reference and shadowring diffuse irradiance for diffuse partly cloudy and direct partly cloudy sky coverage, respectively.

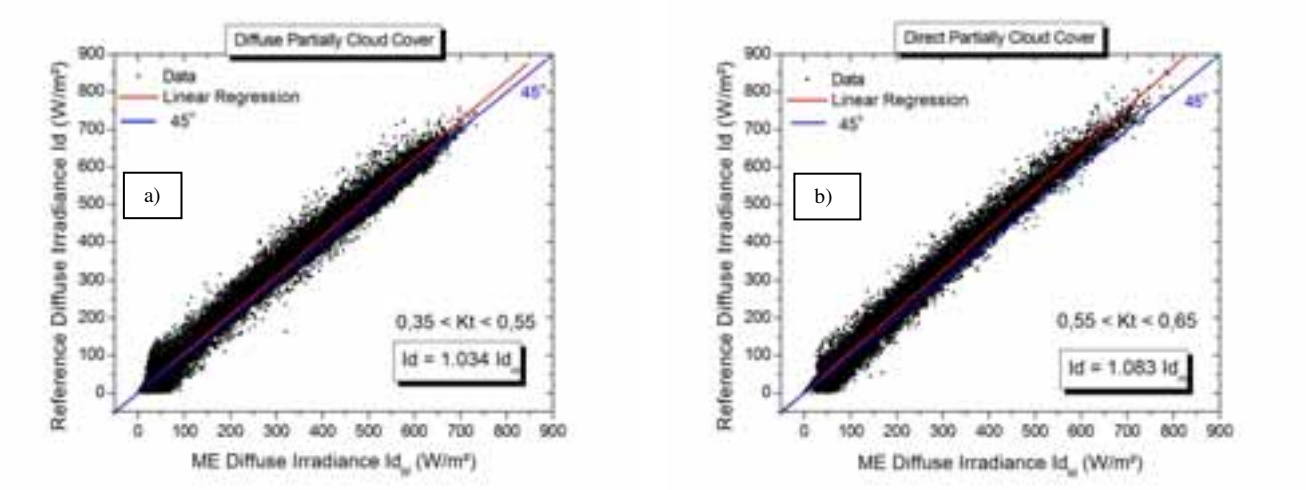

Fig 8. a) Correlation between reference and shadowring diffuse irradiance for diffuse partly cloudy coverage. b) Correlation between reference and shadowring diffuse irradiance for direct partly cloudy sky coverage.

Both in Fig 8a and in Fig 8b, the slope of the correlation between reference and shadowring diffuse irradiance was greater than 1, showing that, on average, the reference diffuse irradiance is greater than the shadowring diffuse value. Therefore, in these coverage, the use of the shadowring method caused an underestimation in the measurement of diffuse irradiance, which increased proportionally as clearness index Kt increased. For diffuse partly cloudy coverage the underestimation was 3.4%, while for direct partly cloudy the underestimation was 8.3%. This underestimation depends on the interaction of radiation with the atmospheric constituents owing to its variable concentrations, quantities and sizes.

Fig 9 shows the correlation between reference and shadowring diffuse irradiance for clear sky.

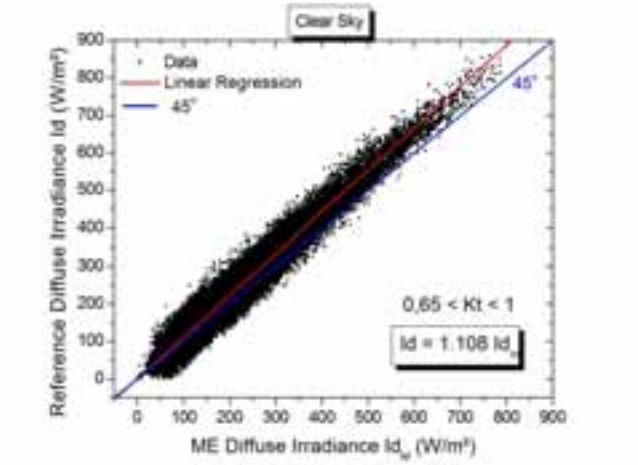

Fig 9. Correlation between reference and shadowring diffuse irradiance for clear sky.

The underestimation of diffuse radiation by use of the ring, which was already occurring to partially cloudy cover, reaches its peak on the clear sky cover. The slope reaches the value 1.108, ie, the shadowring diffuse irradiance is, on average, 10.8% less than the reference diffuse irradiance. As the sky becomes clear, larger particles such as aerosols alter the distribution of scattering of radiation in the atmosphere. Larger particles cause Mie scattering responsible for the effect of anisotropy, ie, the scattering of radiation by the particles start to show directional characteristics, with greater flow directed towards to the surface. This behavior is known as circunsolar radiation and it comes from a small annular area around the solar disk and increases the amount of diffuse radiation incident on the ground (Vartiainen, 1999). Therefore, the circunsolar radiation passes through the atmosphere encapsulated by the direct radiation beam.

Thus, the shadowring also blocks a portion of the circunsolar radiation and thus the diffuse irradiance is less. Therefore, for the clear sky coverage, the ME shadowring method causes the greatest underestimate in the measurement of diffuse irradiance. This justifies the increasing values of the numerical correction factors as increasing the clearness index Kt. In this case we multiply the values of diffuse irradiance by the average factor 1.108.

However, the clear sky conditions may be different depending on the season. In the winter, despite the high transmissivity, the atmosphere is more turbid due to the dry season, with higher concentrations of aerosols. In the summer we have less aerosols due to frequent rains that leave the atmosphere cleaner. Fig 10 shows the correlation between the reference and shadowring diffuse irradiance for January (summer) and July (winter).

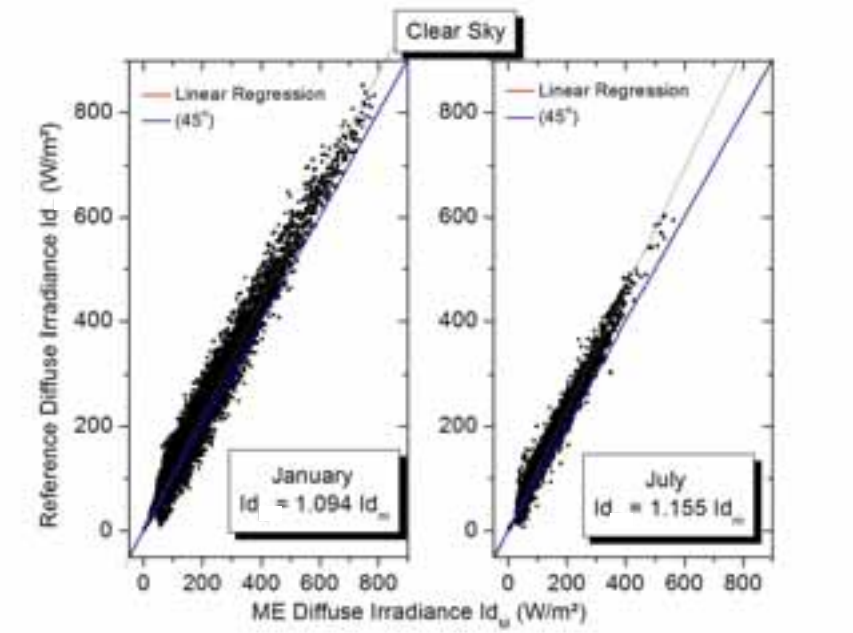

Fig 10. Correlation between the reference and shadowring diffuse irradiance for January (summer) and July (winter).

The numerical correction of 1.094 for January was lower than the correction of 1.155 for July, ie, the shadowring diffuse irradiance for January is 9.4% lower than the reference diffuse irradiance while in July the shadowring diffuse irradiance is 15.5% lower than the reference diffuse irradiance. This fact shows that the effect of anisotropy is higher during winter, where the highest concentration of aerosols provides a greater amount of circunsolar radiation blocked by the ring (Vartiainen, 1999).

4.3. Validation

The evaluation of the corrections was made by means of statistical indicators MBE and RMSE between the reference and the shadowring diffuse irradiances. The first comparison was between the reference and the uncorrected diffuse irradiances. The second comparison was between the reference and isotropic diffuse irradiances (isotropic correction). The third comparison was between the reference and all sky diffuse irradiances (isotropic correction + all sky numerical correction). And finally the fourth comparison was between the reference and the sky cover diffuse irradiances (isotropic correction + sky cover numerical correction). Tab. 4 shows the result of the comparison between the reference and the shadowring diffuse irradiances.

Tab 4. Statistical indicators from the comparison between the reference and the shadowring diffuse irradiances.

Correction Methods	MBE (W/m²)	MBE (%)	RMSE (W/m²)	RMSE (%)
Uncorrected	31,60	24,89	47,12	37,12
Isotropic	5,98	3,93	18,52	12,16
All sky	-1,29	-0,81	16,49	10,35
Sky cover	-1,05	-0,66	14,37	9,00

The diffuse irradiance obtained by the shadowring method without applying any correction underestimates the measurement in 24,89% with 37% of scattering. With the isotropic correction, the difference is around 4% with 12,16% of scattering.

The best results were achieved by combining isotropic and numerical corrections. The use of the all sky numerical correction overestimates the shadowring diffuse irradiance in 0,8% with 10,35% of scattering while the use of the sky cover numerical correction overestimates in just 0.66% the diffuse irradiance with 9% of scattering. So, the use of the ME shadowring method to measure diffuse irradiance requires, besides the isotropic correction, the application of numerical corrections to achieve better results. Fig 11 shows the diffuse irradiance validations for the correction methods with their slopes. The best results occurred for the numerical corrections which showed slopes closer to 1.

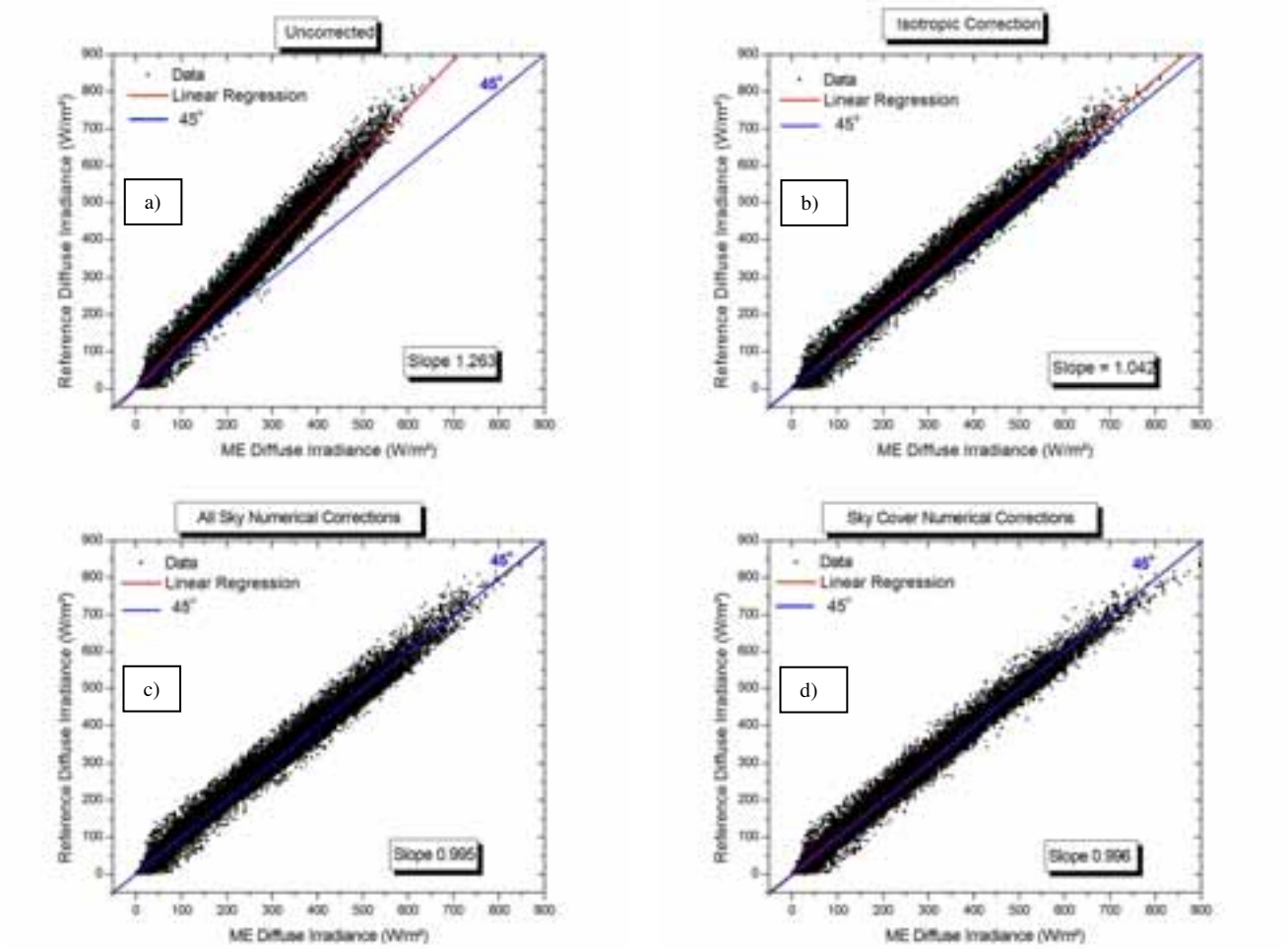

Figure 11.The diffuse irradiance validations for the correction methods. a) Uncorrected. b) Isotropic Correction. c) Isotropic + all aky corrections. d) Isotropic + sky cover corrections

5. Conclusions

The ME shadowring anisotropic corrections proposed as a function of the sky covering (clearness index) were efficient to correct the isotropic diffuse irradiance, approaching the measured and reference diffuse irradiance less than 1%. The results showed that the numerical corrections improve the ME shadowring method, allowing the generation of a reliable global, direct and diffuse radiation database without high financial investments.

6. References

BATTLES, F. J., OLMO, F. J., ALADOS-ARBOLEDAS, L., 1995. On shadowband correction methods for diffuse irradiance measurements. Solar Energy, v.54, n.2, p.105-114.

CODATO, G, OLIVEIRA, A P, SOARES, J, ESCOBEDO, J F, GOMES, E N, DAL PAI, A., 2008. Global and diffuse solar irradiances in urban and rural areas in southeast Brazil. Theor Appl Climatol, v 93, p 57-73.

DEHNE, K., 1984. Diffuse solar radiation measured by the shade ring method improved by a correction formula. Instruments and observing methods, Report n. 15, World Meteorological Organization, p. 263-267.

DRUMMOND, A. J., 1956. On the measurements of sky radiation. Archiv. fur Meteorologie. Geophysik Bioklimatologie, v.7, p.413-436.

ESCOBEDO, J F, GOMES, E N, OLIVEIRA, A P, SOARES, J., 2009. Modeling hourly and daily fractions of UV, PAR and NIR to global solar radiation under various sky conditions at Botucatu, Brazil. Applied Energy, v. 86, p 299-309.

INEICHEN, P, GREMAUD, J M, GUISAN, O, MERMOUD, A., 1984. Study of the corrective factor involved when measuring the difuse solar radiation by use of the ring method. Solar Energy, v.32, p 585-590.

KASTEN, F., DEHNE, K., BRETTSCHNEIDER, W., 1983. Improvement of measurement of diffuse solar radiation. Solar radiation data, série F, n.2, p.221-225, D. Redel, Dordrecht.

KUDISH, A I, EVSEEV, E G., 2008. The assessment of four different correction models applied to the diffuse radiation measured with a shadow ring using global and normal beam radiation measurements for Beer Sheva, Israel. Solar Energy, v.82, p.144-156.

LEBARON, B. A., MICHALSKY, J. J., PEREZ, R., 1990. A simple procedure for correcting shadowband data for all sky conditions. Solar Energy, v.44, n.5, p.249-256.

MELO, J. M. D., ESCOBEDO, J. F., 1994. Medida da radiação solar difusa. In: ENERGÍAS LÍMPIAS EN PROGRESO, VII CONGRESSO IBÉRICO DE ENERGIA SOLAR, Vigo, Espanha. Anais INTERNATIONAL SOLAR ENERGY SOCIETY, v. 1.

OLIVEIRA, A. P., ESCOBEDO, J. F., MACHADO, A. J., 2002. A new shadow-ring device for measuring diffuse solar radiation at surface. Journal of Atmospheric and Oceanic Technology, Boston, v. 19, p. 698-708.

PAINTER, H. E., 1981. The shade ring correction for diffuse irradiance measurements. Solar Energy, v.26, p.361-363.

POLLARD, D. G. e LANGEVINE, L. P., 1988. An anisotropic correction for diffuse irradiance measurements in Guyana. In: Proceeding of the 1988 Annual Meeting, M. J. Coleman (Ed.), p. 238-243, ASES Cambridge.

ROBINSON, H., STOCH, L., 1964. Sky radiation and measurements and corrections. Journal of Applied Meteorology, v.3, p.179-181.

STANHILL, G., 1985. Observations of shade-ring correction factors for diffuse sky radiation measurements at the Dead Sea. Quarterly Journal of the Royal Meteorological Society, v.111, p.1125-1130.

SUEHRCKE, H., McCORMICK, P. G., 1988. The frequency distribution of instantaneous insolation values. Solar Energy, v.40, n.5, p.413-422.

VARTIAINEN, E., 1999. An anisotropic shadow ring correction method for the horizontal di}use irradiance measurements. Renewable Energy, v.17, p.311-317.